JURNAL KIMIA VALENSI
p-ISSN: 2460-6065; e-ISSN: 2548-3013
Journal homepage: https://journal.uinjkt.ac.id/index.php/valensi
Research Article

Nonenzymatic Sensor Based on Glassy Carbon Electrode Modified by Platinum Nanoparticles Decorated Reduced Graphene Oxide for Glucose Detection in Human Urine

Ulfiatun Nisa[1], Dyah Iswantini[1,2], Shahrul Nizam Ahmad[3], Mohd Muzamir Mahat[4], Budi Riza Putra[5], Dinda Iryawati Bedy Saskito[6], Wulan Tri Wahyuni[1,2*]

[1]*Department of Chemistry, Faculty of Mathematics and Natural Sciences, IPB University, Bogor, 16680, Indonesia*
[2]*Tropical Biopharmaca Research Center, International Research Institute of Food, Nutrition, and Health, IPB University, Bogor, 16680, Indonesia*
[3]*School of Chemistry and Environment, Faculty of Applied Sciences, University Teknologi MARA (UiTM), Shah Alam, 40450, Malaysia*
[4]*Green Lithium Recycling Laboratory, Faculty of Applied Sciences, Universiti Teknologi MARA, Shah Alam, 40450, Malaysia*
[5]*Research Center for Metallurgy, National Research and Innovation Agency (BRIN), South Tangerang, Banten, 15315, Indonesia*
[6]*Faculty of Medicine, IPB University, Bogor, 16680, Indonesia*

Email: wulantriws@apps.ipb.ac.id

Article Info
Received: July 6, 2024
Revised: July 8, 2024
Accepted: Nov 18, 2024
Online: Dec 16, 2024

Citation:
Nisa, U., Iswantini, D., Ahmad, S. N., Mahat, M. M., Putra, B. R., Saskito, D. I. B., & Wahyuni, W. T. (2024). Nonenzymatic sensor based on glassy carbon electrode modified by platinum nanoparticles decorated reduced graphene oxide for glucose detection in human urine. *Jurnal Kimia Valensi*, 10(2), 215-228

Doi: 10.15408/jkv.v10i2.40035

Abstract

This research aims to develop a sensitive and selective nonenzymatic electrochemical sensor for glucose detection using a glassy carbon electrode modified with platinum nanoparticles (PtNPs) decorated on reduced graphene oxide (RGO). The structural properties and surface morphology of PtNPs/RGO composite were characterized using Raman spectroscopy and scanning electron microscopy (SEM). In addition, cyclic voltammetry (CV) and differential pulse voltammetry (DPV) techniques were employed to investigate glucose measurements in human urine samples. The developed sensor shows an increasing anodic peak of glucose with a linear response at a concentration range from 10 to 1000 µM, with a detection limit of 5 µM. The proposed sensor also demonstrated good reproducibility, indicated by the value of relative standard deviation (%RSD) of 3.9%, and maintained its current response over seven consecutive measurements. Moreover, the proposed sensor exhibited high selectivity for glucose detection against several potential interferences, such as potassium (K^+), chloride (Cl^-), magnesium (Mg^{2+}), ascorbic acid, dopamine, and urea, with recovery values of 96-102%, which are acceptable within the analytical range. Furthermore, this proposed sensor successfully detected glucose in human urine samples, and their concentrations were not significantly different when measured with a commercial glucose sensor.

Keywords: Electrochemical sensors, glucose, platinum nanoparticles, reduced graphene oxide, water environment.

1. INTRODUCTION

Monitoring the levels of physiological molecules closely related to the body's metabolism is an important stage for disease diagnosis and patient care [1]. These molecules offer essential information about the body's metabolic activities, aiding healthcare practitioners in identifying irregularities and efficiently managing health issues. By consistently evaluating these metabolic indicators, professionals can customize treatments to meet individual requirements, guaranteeing improved health results. The most employed physiological molecular monitoring is blood sugar monitoring in diabetes patients. Diabetes is a metabolic disease characterized by increased blood glucose levels and can cause serious damage to the heart, blood vessels, eyes, kidneys, and nerves [2]. Therefore, the characteristics

of sensor performances such as rapid, high sensitivity, and real-time are paramount parameters for glucose sensors for the early detection of diseases such as diabetes.

Glucose can be measured quantitatively through various methods, including electrophoresis [3], colorimetry [4,5], fluorescence analysis [6], chromatography[7], and electroanalysis [8–12]. Among the methods mentioned above, electroanalysis has been considered a promising method for glucose detection due to its several advantages, including simple measurements, fast response, high selectivity, low cost, and can be used for real-time measurements [13–16].

Electrochemical methods have been widely used to monitor blood sugar levels by taking the patient's blood and then detecting glucose using a stick sensor [17]. However, this method is invasive, painful for the patient, and carries the risk of causing infection because the patient requires repeated examinations every day [18]. Utilizing urine samples presents a non-invasive approach to glucose detection in patients. Elevated blood glucose levels can surpass the renal threshold, causing the kidneys to excrete excess glucose into the urine. This phenomenon, glucosuria, maybe a diagnostic indicator of diabetes or other metabolic disorders [19]. The consumption of foods that are high in sugar or carbohydrates can have a significant impact on glucose levels in both blood and urine [20]. Hence, it is essential to consider dietary intake when evaluating glucose measurements. It is generally recommended to abstain from eating before collecting a sample specimen to ensure accurate glucose level readings. Fasting helps minimize the short-term effects of recent meals, providing a more consistent and fundamental assessment of glucose levels [21]. By implementing this method, the test results can accurately represent the body's metabolic state, free from the immediate effects of food. It allows for a more precise diagnosis and monitoring of metabolic health.

The electrochemical method used in the commercial glucose stick test is an enzymatic-based method that uses glucose oxidase and horse radish peroxidase for glucose detection [22]. However, enzyme-based sensors have been reported to have several shortcomings, including complicated procedures for enzyme immobilization, low stability, and poor repeatability. In addition, the performance of enzyme biosensors is limited by environmental conditions such as pH, temperature, and humidity [15]. Non-enzymatic glucose sensors have emerged as a promising alternative to overcome the limitations of enzymatic sensors. Non-enzymatic sensors have the potential to reduce sensor production costs, improve sensor performance, and increase overall sensor system reliability by eliminating the need for enzymes [23]. However, non-enzymatic sensors still need to improve their selectivity. This is because some sugars can be oxidized in the same potential range as glucose, while electrode performance can be decreased due to ion contamination, especially chloride ions (Cl^-) [24]. Sensitivity and selectivity can be increased by expanding the surface and conductivity of the electrode by modifying it with conductive materials[25].

Several materials have been reported to enhance electrode performance, including metal [26]. Recent research has shown that nanomaterials made of metal have the remarkable ability to imitate the functions of enzymes due to their effective activity as a catalyst for the oxidation reaction of glucose on the surface of an electrode [27]. A study has shown that platinum nanoparticles (PtNPs) can mimic the functionality of peroxidase enzymes in detecting glucose [28]. Apart from metal-based nanomaterials, carbon-based nanomaterials have also been widely used to develop electrochemical sensors [29]. One carbon nanomaterial that has been widely used is graphene. Graphene is an allotrope of carbon in the form of a single two-dimensional graphite layer, arranged hexagonally, sp^2 bound, and very stable. The oxidation process of graphene will produce a new compound called graphene oxide (GO), which has many carboxyl, hydroxyl, and epoxy functional groups and is very well dispersed in water. This nanomaterial has several advantages, including having a high theoretical specific surface area, good conductivity, and stability at room temperature [30]. The use of carbon nanomaterial, namely reduced graphene oxide (RGO) as a sensor, has been previously reported and proven to increase the conductivity of the electrode surface [31,32].

Nevertheless, regarding the advantages of modifying materials that can be used to improve electrode performance, this is the first time anyone has reported the usage of platinum nanoparticles (PtNPs) and RGO to be employed for the fabrication of non-enzymatic glucose sensors in human urine. Therefore, we proposed the development of a non-enzymatic electrochemical sensor for glucose detection using a carbon-based electrode modified with RGO and PtNPs that can be used for non-invasive glucose detection in human urine. By utilizing urine as a sample, we can achieve reliable glucose monitoring without the associated discomfort and risks of blood sampling. This paper highlights the potential of urine-based glucose detection, presenting a non-invasive technique that maintains high accuracy and sensitivity, comparable to commercial sensors.

2. RESEARCH METHODS

Materials and instruments

The chemicals used in this research, such as glucose, graphite powder, $KMnO_4$, H_2SO_4, K_2PtCl_4, NaOH, dopamine, $MgSO_4$, and urea, were obtained from Sigma Aldrich. H_2O_2, $K_3Fe(CN)_6$, and HCl were purchased from Merck, while KCl and ascorbic acid were obtained from HiMedia. The equipment used in this

research consisted of Palmsens Emstat3 potentiostat (ES316U669), electrode compartments and connectors, Field Emission Scanning Electron Microscope (FE-SEM) (Apreo 2 Thermo Scientific), Raman spectroscopy (HORIBA HR Evolution Raman Microscopes), sonicator, EasyTouch® GCU and computer with PSTrace 5.9 software (Palmsens), OriginPro 2018 (OriginLab, Northampton), general laboratory glassware, and analytical balance.

2.1. Synthesis of Graphene Oxide (GO)

GO was synthesized from graphite using a Hummer method with some modifications [33]. Briefly, 1 g of graphite and 0.5 g of $NaNO_3$ were mixed with 25 mL of H_2SO_4 and stirred for 1 hour at 0 °C. Then, 3 g of $KMnO_4$ was slowly added while maintaining the temperature below 20 °C and stirred for 1 hour. The solution was left at room temperature (25 °C) for 30 minutes. Subsequently, 50 mL of water was slowly added, raising the temperature to 90-95 °C. The mixture was stirred for 1 hour and left to rest for 15 minutes. Next, 50 mL of 30% H_2O_2 was added to stop the reaction, and the mixture was stirred for another hour. The resulting GO was filtered, washed with distilled water, and dried in an oven at 80 °C for 8 hours. The obtained product was then analyzed using Raman spectroscopy.

2.2. Synthesis of Reduced Graphene Oxide (RGO)

Graphene oxide (GO) was reduced to reduced graphene oxide (RGO) using the previous method[34]. Initially, 400 mL of distilled water was combined with 400 mg of GO and subsequently added with 4 g of ascorbic acid. The solution was stirred with a magnetic stirrer for 30 minutes at 60 °C. The resulting product was centrifuged at 3800 rpm for 40 minutes to remove the supernatant. To oxidize any remaining ascorbic acid, an excess of 30% H_2O_2 was added to the filtrate, and the mixture was stirred for an additional 30 minutes at 60 °C. The precipitate was separated from the supernatant again by centrifugation at 3800 rpm for 40 minutes. Afterward, the filtrate was washed using ethanol in three replicates and with distilled water and dried at 120 °C for 24 hours. The final product was analyzed using Raman spectroscopy.

2.3. Modification of GCE with RGO/PtNPs

The surface of a glassy carbon electrode (GCE) as a working electrode was modified with 4 µL RGO (1 mg/mL in water). Then, platinum electrodeposition was performed by cyclic voltammetry (CV) technique at the potential range from +1 V to -0.3 V vs. Ag/AgCl for 20 cycles with a scan rate of 100 mV s^{-1} using 5 mM K_2PtCl_4 solution in 0.5 M H_2SO_4 as an electrolyte solution. The electrode was then defined as a glassy carbon electrode modified with platinum decorated on reduced graphene oxide (GCE/RGO/PtNPs).

2.4. Evaluation of Electrochemical Behaviour of Glucose at Modified Electrode

Electrochemical impedance spectroscopy (EIS) was used to study the electrochemical behavior of glucose on GCE/RGO and GCE/RGO/PtNPs. For the EIS evaluation, a 1 mM $K_3Fe(CN)_6$ solution in 0.1 M KCl was prepared, and the resistance was measured. EIS analysis of the electrode was performed in several experimental parameters such as equilibrium time (3 s), scan type (fixed), E_{ac} (0.01 V), and frequency range (1 to 10^6 Hz). To analyze EIS results, an equivalent Randles circuit consisting of a resistor and a capacitor was constructed to interpret the interfacial phenomena on the electrode/electrolyte interface. This equivalent circuit was employed to determine the resistance values of the electrode and the solution through a suitable fitting mode.

Then, the electrochemically active surface area (ECSA) of GCE/RGO/PtNPs was determined by measuring 1 mM $K_3[Fe(CN)_6]$ solution in 0.1 M KCl using the CV technique. The employed potential in this CV technique in the window ranges from +0.8 to -0.8 V vs. Ag/AgCl. The scan rates used in this CV technique were varied at 25, 50, 100, 150, 200, and 250 mV/s to determine the ECSA of the modified electrode.

Meanwhile, the diffusion coefficient of GCE/RGO/PtNPs was determined by measuring glucose solution in the concentration range of 0.1 mM to 1 mM using the chronoamperometry technique. The experimental parameters used in this technique involved an applied potential of 0 V and a scan time of 120 s.

Next, glucose measurements were investigated using the square wave voltammetry (SWV) technique with three modified electrodes (bare GCE, GCE/RGO, and GCE/RGO/PtNPs). A solution of 10 mM glucose in 0.1 M NaOH was prepared and employed for glucose measurements using square wave voltammetry at a frequency of 10 Hz, a potential step of 5 mV, and a range of potential window from -0.6 to +0.1 V vs. Ag/AgCl.

2.5. Analytical performance of GCE/RGO/ PtNPs

The analytical performance of GCE/RGO/PtNPs in glucose sensing was evaluated in several parameters, including linearity, limit of detection (LOD), limit of quantitation (LOQ), reproducibility, stability, and selectivity.

Linearity

The glucose solution was prepared in the concentration range from 0.1 to 1 mM using 0.1 M NaOH as an electrolyte. The glucose measurements were carried out using the SWV technique at a frequency of 10 Hz, a potential step of 5 mV, and the range of potential window from -0.6 to +0.1 V vs Ag/AgCl. Linearity was analyzed using the calibration curve created from glucose concentration as the *x*-axis and glucose oxidation current as the *y*-axis. Thus, the coefficient of

determination (R^2) obtained from linearity studies can be determined as the highest sensitivity indicated by $R^2 \approx 1$. In addition, LOD and LOQ were calculated based on the ratio of signal-to-noise, with the LOD value estimated at 3:1 and LOQ at 10:1.

Reproducibility, Stability, and Selectivity

Reproducibility was evaluated by preparing six modified electrodes based on GCE/RGO/PtNPs and employing them to measure 1 mM glucose in 0.1 M NaOH in triplicate experiments. Meanwhile, the stability of GCE/RGO/PtNPs was investigated by measuring 0.1 M NaOH containing 1 mM glucose using a similar electrode for 7 consecutive measurements. In addition, the selectivity of GCE/RGO/PtNPs was studied by measuring 1 mM glucose in 0.1 M NaOH in the presence of several interfering species such as ascorbic acid, dopamine, urea, and magnesium in the concentration ratio of 1:1. All electrochemical measurements were carried out using SWV technique at a frequency of 10 Hz, potential step of 5 mV, and the range of potential window from -0.6 to + 0.1 V vs. Ag/AgCl.

2.6. Applicability of GCE/RGO/PtNPs for glucose detection in human urine samples

Urine samples were taken from 5 healthy volunteers after fasting for approximately 8 hours (consuming only water) before sample collection. The samples were then collected in sterile containers, individually packaged, and labeled. This procedure was approved by the Human Research Ethics Committee of the Bogor Agricultural University with Ethical approval number 175/IT3.KEPMSM-IPB/SK/2024. Then, the human urine samples were diluted 5 times in 0.1 M NaOH with the addition of glucose and diluted to a final volume of 10 mL. The obtained concentrations of glucose solution were 60, 80, 100, 200, 400, and 600 μM. Then, an electrode based on GCE/RGO/PtNPs was applied to measure the glucose concentration in human urine samples using the SWV technique with the standard addition method. The obtained results from the proposed sensors were then compared with a commercial glucose check kit as a reference method and subsequently analyzed using a statistical analysis (*t*-Student test) at a 95% confidence interval.

3. RESULTS AND DISCUSSION

3.1. Characterization of the surface of the modified electrode using Raman and FESEM

Figure 1A shows the obtained Raman spectra for 3 different materials, e.g., graphite, GO, and RGO, indicating three prominent peaks associated with the characteristics of carbon-based nanomaterials. The first peak, the D band, corresponds to the breathing modes of sp2 atoms in graphene and requires a defect for its activation, often indicating the presence of disorder or defects in the graphene structure [35]. The G band originates from the C-C stretching of sp^2 hybridized carbon in the graphite material structure. The 2D peak is equivalent to the number of stacked graphene layers [36]. The 2D band detected in graphite was not observed in either GO or RGO, indicating successful exfoliation of the graphene layer into GO and RGO. Additionally, the intensity ratio of the D/G (I_D/I_G) band decreased to 1.13 in RGO compared to GO, due to the removal of functional groups and the restoration of the graphene layer structure. In addition, based on Figure 1A, the I_D/I_G ratio for RGO/PtNPs shows a slight decrease compared to RGO, suggesting that the PtNPs are decorated on the RGO without altering its planar structure [37].

Figures 1B and 1C show the surface morphology of RGO and RGO/PtNPs obtained from SEM-EDS analysis. The RGO structure in **Figure 1B** displays several crumpled nanosheets of graphene layers, while the presence of PtNPs spheres on the surface of the RGO sheet was obtained via the electrodeposition method as shown in **Figure 1C**. This observation is consistent with previous reports that electrodeposited PtNPs typically exhibit a round shape [38]. Additionally, the EDS spectrum confirmed the presence of platinum, indicating the successful electrodeposition of PtNPs on the electrode surface. The average size of the PtNPs was measured to be 51.36 nm. This size is quite similar to previous studies reported electrodeposited Pt nanoparticles with average sizes ranging from 30 to 50 nm on reduced graphene oxide, demonstrating that nanoparticles can be effectively utilized for catalytic applications [39]. The impact of nanoparticle size on catalytic performance is well-documented. Smaller PtNPs generally offer higher surface area-to-volume ratios, leading to more active sites and improved catalytic efficiency. Conversely, larger PtNPs, while potentially offering fewer active sites, can provide enhanced stability and are less prone to agglomeration, which can benefit specific electrochemical applications.

3.2. Electrodeposition PtNPs on GCE/RGO

Platinum nanoparticles (PtNPs) were synthesized using electrodeposition techniques, specifically cyclic voltammetry, which was carried out for 20 cycles. **Figure 2A** illustrates the electrodeposition process of PtNPs on the GCE/RGO surface. During the initial cycle, a faint reduction peak associated with the reduction of platinum was observed. As the cycle progressed, the peak intensity increased, and at the 20th cycle, a pair of well-defined oxidation and reduction peaks were observed at -0.19 V vs Ag/AgCl. This phenomenon is due to hydrogen's adsorption and desorption processes on the Pt particles [40]. In addition, an anodic peak at 0.29 V vs Ag/AgCl was observed. This peak indicates an irreversible reaction, facilitating platinum material's continuous nucleation and growth on the electrode surface [41]. The appearance of these redox

peaks indicates that the deposition of Pt has been successfully achieved. The significant increase in peak current reduction with each cycle indicates the progressive accumulation of PtNPs, which increases the electroactive surface area of the electrode. The larger surface area provided by the deposited PtNPs is essential for improving the electrocatalytic performance of the electrode.

3.3. Electrochemical impedance spectroscopy (EIS) analysis of the modified electrode

Electrochemical impedance spectroscopy (EIS) was performed to evaluate the electrochemical properties of the bare and modified electrodes, as shown in **Figure 2B**. Nyquist plots were obtained for (a) bare GCE, (b) GCE/RGO, and (c) GCE/RGO/PtNPs in a solution of 1 mM $K_3Fe(CN)_6$ in 0.1 M KCl within a frequency range from 10^6 kHz to 1 kHz and an AC amplitude of 10 mV at the open circuit potential (OCP). The Nyquist plots 2 shows the fitted impedance data used to estimate the solution resistance (R1), charge-transfer resistance (R2), and double-layer capacitance (C1). Figure 2B shows that the bare GCE exhibited the highest R2 value (261.43 Ω), indicating poor electron transfer. When the GCE was modified with reduced graphene oxide (RGO), the R2 value significantly decreased to 157.51 Ω, showing improved electron transfer due to the highly conductive nature of RGO. Finally, the GCE/RGO/PtNPs electrode had the lowest R2 value of 84.40 Ω, indicating the best electron transfer performance. This drastic reduction in charge transfer resistance can be attributed to the excellent conductivity of RGO and the catalytic properties of the PtNPs, which collectively facilitate faster electron transfer. The improved electron transfer kinetics of GCE/RGO/PtNPs is crucial for efficient glucose sensing, as it directly impacts the electrode sensitivity and response time. The combination of RGO, which enhances the overall conductivity, and PtNPs, which act as electrocatalysts, creates a highly efficient platform for glucose electrooxidation.

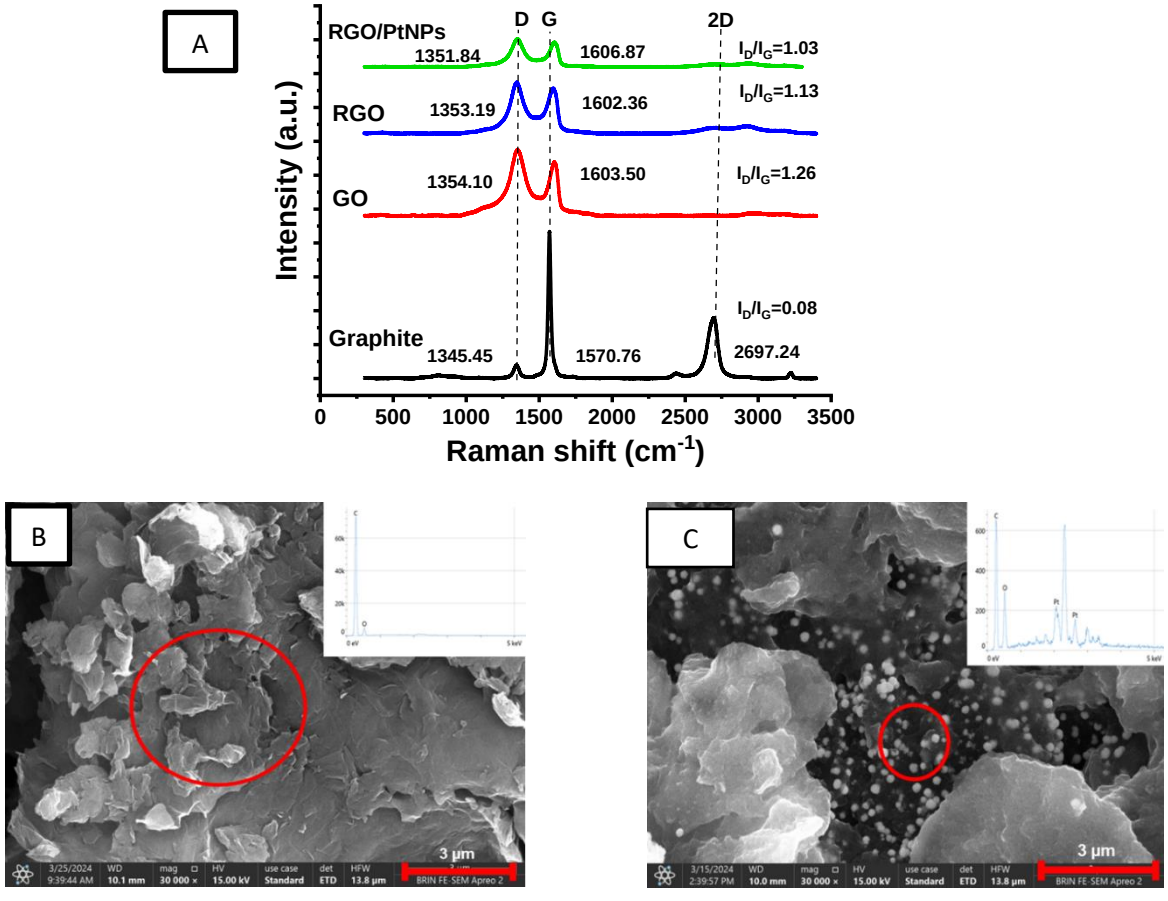

Figure 1. Raman spectra of (A) graphite, GO, and RGO, (B) RGO and RGO/PtNPs. FESEM images of (B) RGO and (C) RGO/PtNPs.

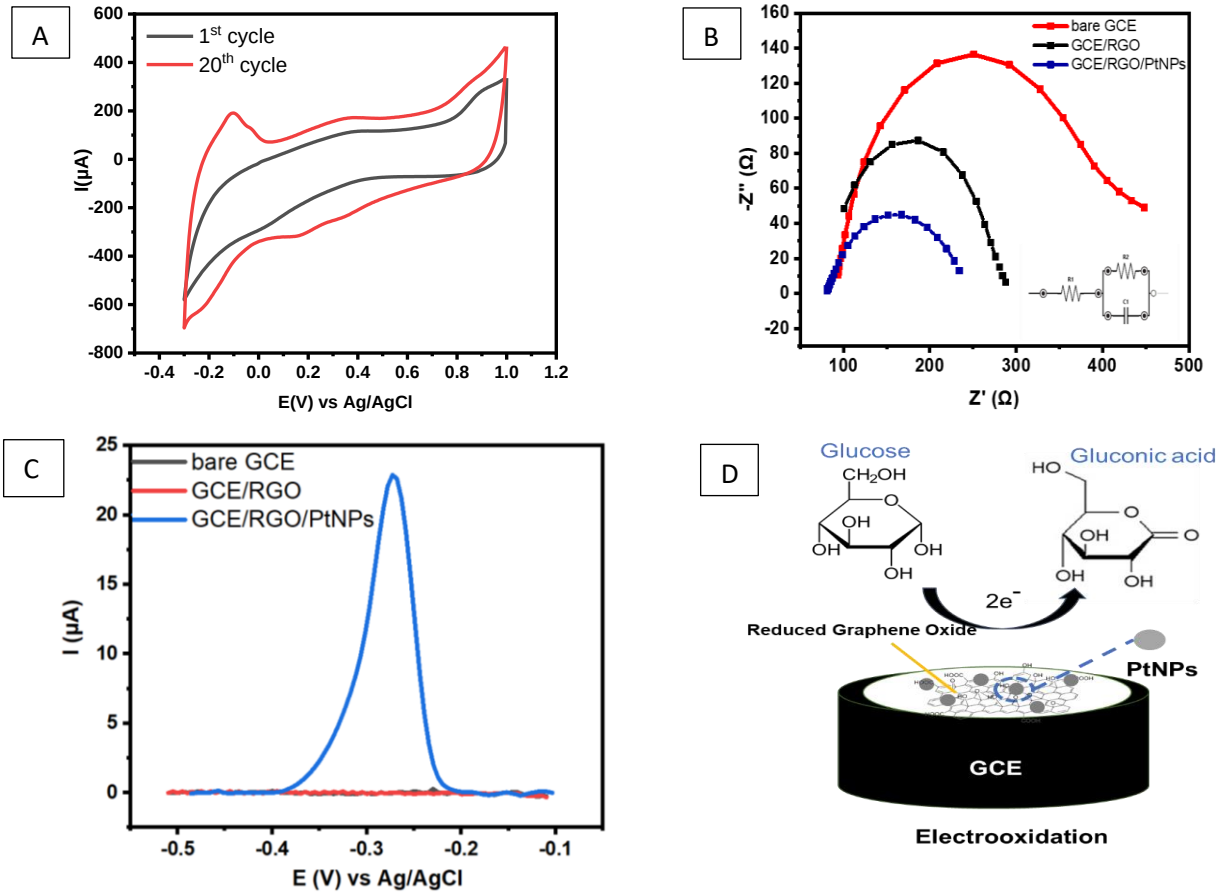

Figure 2. (A) Voltammograms of 5 x 10^{-3} M K_2PtCl_4 in 0.5 M H_2SO_4 at a scan rate of 100 mV s^{-1} using GCE/RGO, (B) Nyquist plot at a frequency range of 10^5 kHz to 5 kHz with an AC amplitude of 0.01 V at the open circuit potential (OCP) in 0.1 M KCl containing 1 mM $K_3[Fe(CN)_6]$ for the bare GCE, GCE/RGO, and GCE/RGO/PtNPs, (C) Squarewave voltammograms of 10 mM glucose in 0.1 M NaOH solution using three different electrodes: bare GCE, GCE/RGO, and GCE/RGO/PtNPs. The voltammograms were recorded at a frequency of 10 Hz, with a potential step of 5 mV, and a potential window from -0.6 to +0.1 V versus Ag/AgCl, and (D) Schematic illustration of the anodic oxidation process of glucose at surface of GCE/RGO/PtNPs

3.4. Electroanalytical Behavior of the Modified Electrode for Glucose Detection

The electrochemical behavior of the bare GCE and the modified electrodes was evaluated using square wave voltammetry (SWV) in the potential range from -0.6 V to 0.1 V vs. Ag/AgCl. Square Wave Voltammetry was selected due to its superior sensitivity and ability to detect low-concentration analytes such as glucose, even in complex matrices. Compared to other voltammetric techniques, SWV provides enhanced signal-to-noise ratios, making it highly suitable for detecting subtle changes in the electrochemical behavior of modified electrodes. This technique allows for rapid data collection and produces clear, well-resolved peaks, facilitating the identification of oxidation and reduction processes. In particular, SWV is ideal for studying glucose oxidation because it allows for the precise measurement of electron transfer kinetics associated with glucose electrooxidation [42]. These characteristics make SWV the optimal choice for analyzing the enhanced electrochemical activity of the GCE/RGO/PtNPs electrode in this study. **Figure 2C** shows the SWV response for glucose detection on three electrodes: bare GCE, GCE/RGO, and GCE/RGO/PtNPs. A clear oxidation peak at -0.275 V vs Ag/AgCl is observed only with the GCE/RGO/PtNPs electrode. In contrast the bare GCE and GCE/RGO electrodes did not exhibit an anodic oxidation peak within the measured potential range. Platinum metal has previously been reported to catalyze the electrooxidation of glucose to gluconic acid [23,43]. The synergistic effect between the conductive properties of reduced graphene oxide (RGO) and the electrocatalytic properties of PtNPs enhances the electron transfer during glucose oxidation. This synergy results in a higher current response and improved the GCE/RGO/PtNPs electrode sensitivity.

Furthermore, **Figure 2D** provides a schematic illustration of the anodic oxidation process of glucose on the surface of the GCE/RGO/PtNPs electrode. The illustration demonstrates how the presence of PtNPs

facilitates glucose oxidation, leading to gluconic acid formation and the release of electrons. The conductive nature of RGO ensures efficient electron transfer from the glucose oxidation process, further amplifying the signal. Thus, the GCE/RGO/PtNPs electrode is a highly effective platform for glucose detection, combining the electrocatalytic activity of PtNPs with the excellent conductivity of RGO. This modification significantly lowers the charge-transfer resistance and increases the electrochemical performance, as demonstrated in the Nyquist plots from electrochemical impedance spectroscopy (EIS) analysis. Thus, GCE/RGO/PtNPs were selected for further studies to investigate the electrooxidation process of glucose.

The electrochemically active surface area (ECSA) of bare GCE and GCE/RGO/PtNPs can be investigated by obtaining a voltammogram in a different scan rate against the anodic current of compound $K_3[Fe(CN)_6]$. **Figures 3A and 3B** show the cyclic voltammogram of 5 mM $K_3[Fe(CN)_6]$ in 0.1 M KCl measured with bare GCE and GCE/RGO/PtNPS. The insets in these figures show the linear relationship between the scan rate and the oxidation and reduction currents of 5 mM $K_3[Fe(CN)_6]$ in 0.1 M KCl measured with bare GCE and GCE/RGO/PtNPs. Thus, the ECSA of bare GCE and GCE/RGO/PtNPs were determined using the Randles-Sevcik equation [44]:

$$I_p = (2.69 \times 10^5)\, AD^{1/2} n^{3/2} v^{1/2} C \qquad (1)$$

where I_p is the peak current for the oxidation or reduction of $K_3Fe(CN)_6$ (Ampere), n is the number of electrons involved in the redox reaction of $K_3[Fe(CN)_6]$ (1), D is the diffusion coefficient, A is the effective area electrode (cm^2), v is the scan rate ($V\ s^{-1}$), and C is the concentration of $K_3[Fe(CN)_6]$ solution ($mol\ cm^{-3}$).

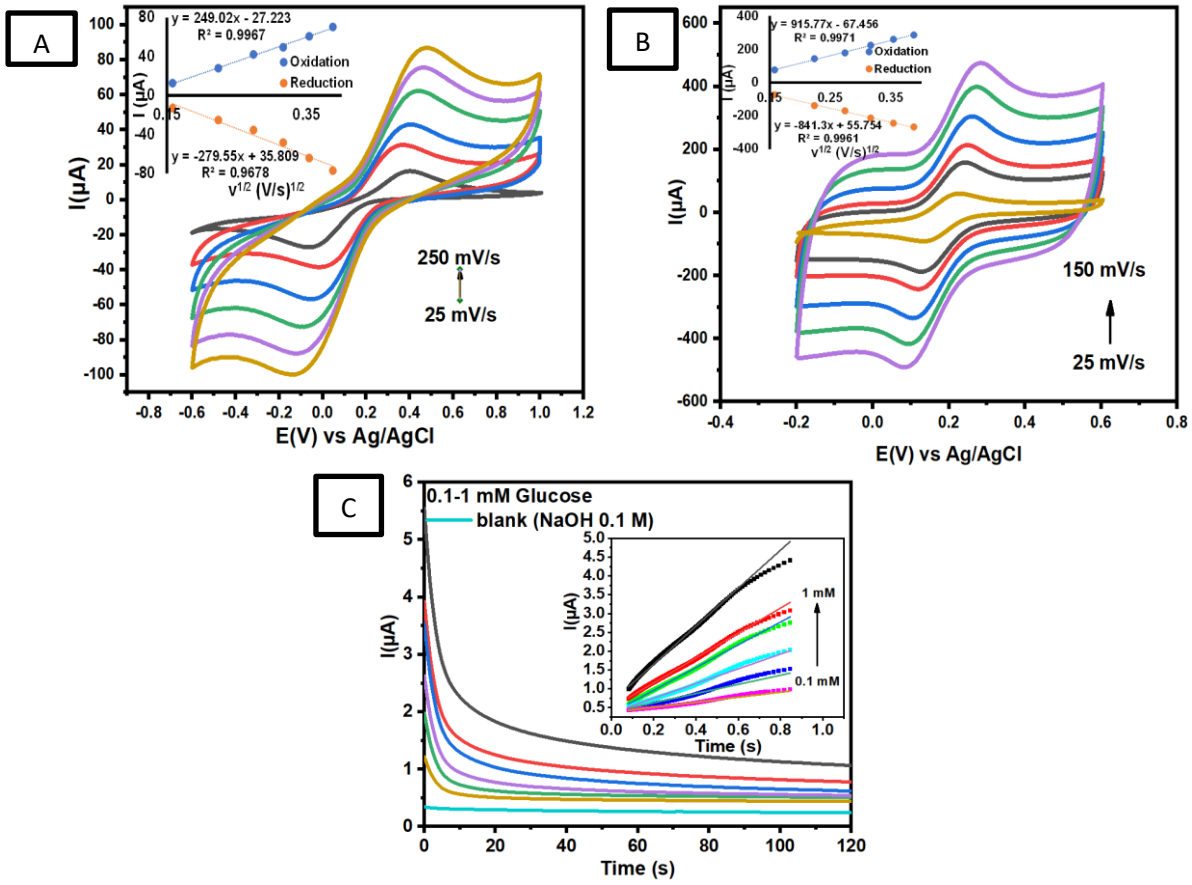

Figure 3. Cyclic voltammogram of 5 mM $K_3[Fe(CN)_6]$ in 0.1 M KCl measured with (A) bare GCE and (B) RGO/PtNPS modified GCE. (inset: The linear relationship between scan rate and Oxidation and reduction current of 5 mM $K_3[Fe(CN)_6]$ in 0.1 M KCl) (C) Amperometric response of 0.1 M NaOH and glucose in NaOH at various concentrations measured with GCE/RGO/PtNPs

The results obtained indicate that the ECSA of the bare glassy carbon electrode (GCE) is 0.08 cm², while that of the GCE modified with reduced graphene oxide (RGO) and platinum nanoparticles (PtNPs) is 0.26 cm². This significant threefold increase demonstrates that modification with RGO/PtNPs substantially enhances the effective area. This result confirms that the surface modifications of GCE with RGO/PtNPs provide more active sites for electrochemical reactions for the oxidation and reduction process. Previous studies reported similar enhancements in the ECSA or effective surface area using GCE modified with PtNPs and RGO, which improved the sensitivity and performance of the electrode for the simultaneous detection of electroactive molecules [45]. Another study also observed substantial increases in the effective surface area with rGO/PtNPs-modified electrodes, facilitating improved electrochemical detection of Fe(II) [46]. This enhancement can be attributed to the high surface area and excellent conductivity of RGO combined with the catalytic properties of PtNPs, which create a more efficient platform for electrochemical sensing. Such modifications are critical for developing high-performance sensors, as they directly impact the electrode's ability to facilitate faster electron transfer and higher sensitivity, which is essential for applications requiring precise and reliable measurements.

To further investigate the sensor performance, the diffusion coefficient for glucose was determined using the amperometric method by increasing the glucose concentration from 0.1 – 1 mM (Figure 3C). Then, the diffusion coefficient (*D*) of GCE/RGO/PtNPs for glucose measurements can be calculated using the Cottrell equation[44] as follows:

$$I = nFAD^{1/2} C_b \pi^{-1/2} t^{-1/2} \quad (2)$$

where *I* is the peak current for the oxidation or reduction of glucose (Ampere), *n* is the number of electrons involved in the redox reaction of glucose (2), where *F* is Faraday's constant (96500 C mol^{-1}), *A* is the electrode surface area (cm^2), *D* is the analyte diffusion coefficient (cm^2 s^{-1}), and C_b is the analyte concentration (mol cm^{-3}). The diffusion coefficient for glucose measurement was determined using GCE/RGO/PtNPs in alkaline conditions, resulting in a value of 3.18 x 10^{-6} cm^2 s^{-1}. This value is slightly lower than the diffusion coefficients reported in previous studies. Previous studies reported a diffusion coefficient of 8 x 10^{-6} cm^2 s^{-1} using a GC/Ni electrode [47], and 6.49 x 10^{-6} cm^2 s^{-1} with a cobalt hydroxide-modified glassy carbon electrode[48]. The discrepancies can be attributed to several factors related to the experimental conditions, including temperature, electrolyte concentration, and viscosity. The unique catalytic properties of the GCE/RGO/PtNPs electrode may also influence the glucose diffusion process. Factors such as surface area, electrode porosity, and interactions between the modified surface and glucose could also affect the diffusion rate. We noted that a higher diffusion coefficient correlates with increased mass transport and reaction kinetics on the electrode surface, while the opposite is valid for a lower diffusion coefficient [49–51].

3.5. Analytical Performance of GCE/RGO/PtNPs

Figure 4A show glucose measurements with GCE/RGO/PtNPs showed a linear relationship at concentrations of 10-100 µM and 100-1000 µM with the equation I_p (µA) = 0.0254$C_{Glucose}$ (µM) + 1.3175; R^2 = 0.9951 and I_p (µA) = 0.0084$C_{Glucose}$ (µM) + 2.9443; R^2 = 0.991. Thus, it can be calculated the values of LOD and LOQ for glucose measurement were 5 µM and 10 µM, respectively. These values are below the maximum limits for normal glucose levels in human urine (10 mM)[52], indicating that the developed sensor has the potential for application to real samples [53]. Meanwhile, stability was evaluated by performing repeated measurements using a single modified electrode. The results demonstrate that a relative standard deviation (%RSD) of less than 5%, specifically 3.8%, was achieved by the seven consecutive measurements for glucose detection (**Figure 4B**). Reproducibility was evaluated by measuring glucose with 5 individual modified electrodes and obtained %RSD values lower than 5% (**Figure 4C**). The selectivity of the GCE/RGO/PtNPs sensor was evaluated in the presence of ions such as K^+, Mg^{2+}, and Cl^- as well as organic molecules such as ascorbic acid, urea, and dopamine. The obtained result showed that glucose measurements were not influenced by the presence of several potential interfering species, indicated by the values of recovery percentage within the acceptable analytical range (Figure 4D) [54]. The electrochemical performance of GCE/RGO/PtNPs can be compared with previously reported electrochemical sensors (**Table 1**). This comparison highlights the effectiveness of the GCE/RGO/PtNPs sensor in achieving low detection limits and maintaining reliable performance across multiple evaluations.

3.6. Real samples analysis

The determination of glucose in urine samples was performed using the standard addition method by adding standard glucose concentrations (0, 60, 80, 100, 200, 400, and 600 µM) to the urine samples, followed by electrochemical measurement using the SWV method on the GCE/RGO/PtNPs sensor. The results were compared with those obtained using a commercial glucose kit sensor, as shown in Table 2. Additionally, voltammograms for the original

urine samples and those spiked with glucose were recorded, and a linear relationship between glucose concentration and current was established (Figure 5A and 5B). A statistical study was conducted to evaluate the performance of the developed sensor compared to the commercial kit. The glucose levels measured by the two methods were then compared at a 95% confidence level, and no significant difference was found between the two methods of measurement. The results revealed that the t-statistic value of -1.07 did not exceed the critical t-value of 2.30, indicating no statistically significant difference between the sensor and the commercial kit for determining glucose in urine. These findings suggest that the proposed sensor has the potential to be utilized on actual urine samples and can be further developed for routine urine glucose detection.

Multiple investigations have confirmed the precision and dependability of urine glucose detections, emphasizing their robust association with blood glucose levels, particularly in cases of high blood sugar. The previous research reported that a flexible graphene paper modified with Pt and Pd alloy nanoparticles was able to assess glucose levels consistently in urine samples in clinical environments, and the results were similar to those of blood glucose[60]. Another study showed that —Cu(II)-Ni(II)/SBA-15 sensor had excellent sensitivity and specificity when tested in artificial human blood serum and urine [57]. A recent study has further emphasized the specificity of nonenzymatic glucose sensors. Comparative studies on the selectivity of sensors in blood and urine samples have demonstrated that blood samples exhibit high selectivity in the presence of fewer interfering compounds. However, urine samples can reach equivalent selectivity through improved sensor designs. As an illustration, previous studies found that their Pt nanoparticles/SWCNTs/NiO ternary nanocomposite sensor exhibited exceptional selectivity in blood and urine samples, with low disruption from other prevalent biomolecules [62]. The appropriate design and a careful choice of material for the fabrication of nonenzymatic sensors can maintain a high level of selectivity and accuracy when used with various sample types.

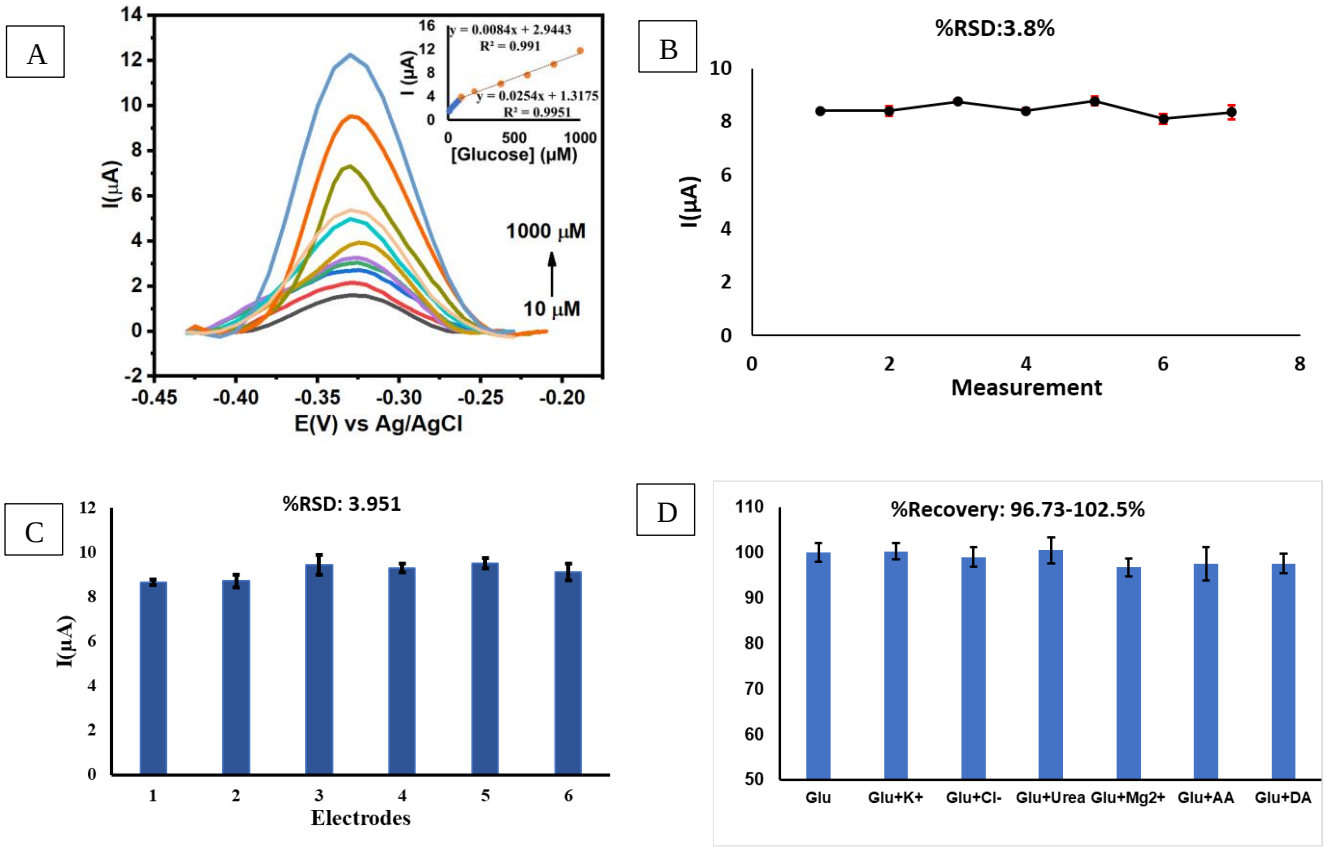

Figure 4. (A) Voltammogram obtained at a scan rate of 50 mV s^{-1} for the various concentrations of glucose from 10 – 1000 µM in NaOH 0.1 M (inset: The linear relationship between various concentrations of glucose against their oxidation current), (B) The current response of 1 mM glucose in 0.1 M NaOH measured with GCE/RGO/PtNPs in 7 consecutive measurements, (C) The current intensity of glucose oxidation of 1 mM in NaOH 0.1 M in 6 different GCE/RGO/PtNPs individuals, (D) %recovery for the determination of glucose (1 mM) in the presence of several interferents, AA (Ascorbic Acid), DA (Dopamine), ion K^+, $Mg^{2+,}$ and Cl^-

Table 1. Comparison of GCE/RGO/PtNPs with other modified electrodes for glucose detection

Electrode	Linear range (µM)	LOD (µM)	Samples	Ref
Pt/Ni@rGO	2 - 5000	6.3	Commercial beverages	9
PtNPs/CNTs	28 - 46600	28.0	-	55
Nickel carbide	2 - 10000	0.5	Blood, Urine	56
Cu(II)-Ni(II)/SBA-15	10 - 1000	2	Artificial Human Blood Serum, Urine	57
2D-MoS_2 nanostructures	1 - 500	0.1	Urine	58
La0.6Sr0.4Co0.8Fe0.2O3 and La1.7Sr0.3CuO4	0.5 - 100	0.1	Synthetic Urine	59
Pt&Pd alloy nanoparticles	0.5 - 500	0.05	Urine, Fingertip Blood	60
GQDs/Fe_3O_4/polypyrrole nanocomposite	1 - 100	0.2	Blood, Urine	61
PtNPs/SWCNTs/NiO	50 - 2700	2.16	Blood	62
RGO/PtNPs	10 - 1000	5	Urine	**This work**

* CNTs:carbon nanotubes, SWCNTs:single-wall carbon nanotubes

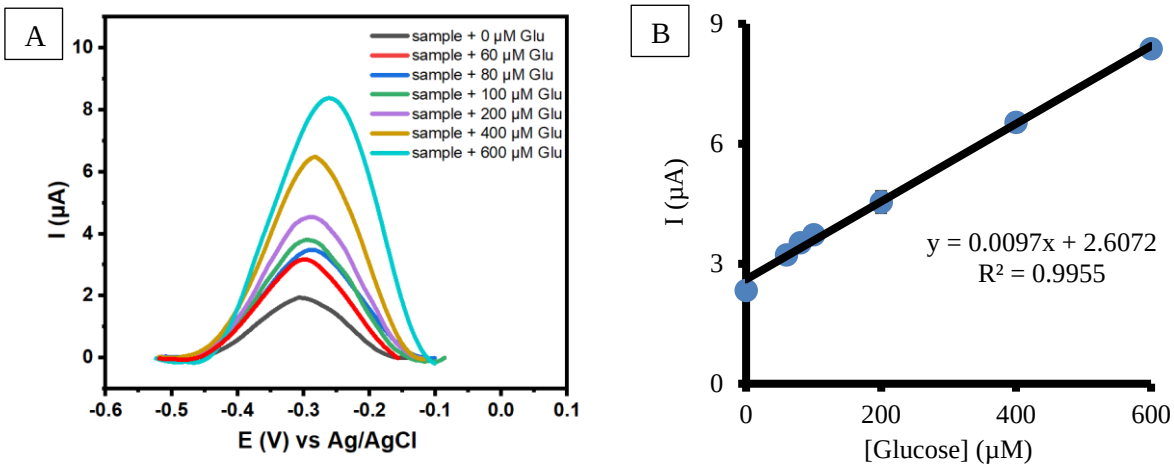

Figure 5 (A) Voltammogram obtained at a scan rate of 50 mV s^{-1} for urine samples with various added glucose concentrations ranging from 0 to 600 µM in 0.1 M NaOH, (B) The linear relationship between glucose concentration and their corresponding oxidation current

Table 2. Subjects' glucose levels were measured using GCE/RGO/PtNPs vs commercial glucose urine kit

Subject	Electrochemical method (mM)	Glucose kit (mM)	t-test	
			t-statistic	t-table
1	2.61	3.03		
2	2.42	2.90		
3	3.19	3.53	-1.07	2.30
4	1.32	1.86		
5	2.25	2.67		

4. CONCLUSIONS

Our research demonstrates that noninvasive glucose detection using a nonenzymatic electrochemical sensor has been successfully developed using an electrode modified with RGO/PtNPs. The sensor shows high sensitivity with a linear response over a wide measurement range, low detection limit (LOD), high reproducibility, and selectivity. It has also been successfully applied to detect glucose in human urine samples, achieving performance comparable to commercial glucose sensors. Using urine as a sample offers advantages such as ease of collection, reduced discomfort, and the potential for frequent monitoring without invasive procedures. The incorporation of platinum nanoparticles (PtNPs) as an electrocatalyst significantly enhances the electron transfer process for glucose oxidation, improving the sensor's overall performance. The synergy between RGO, known for its electrical conductivity, and PtNPs provides a promising platform for glucose sensing, showing excellent stability and precision. Future research could

explore miniaturizing the sensor for portable devices, ensuring long-term stability, and extending its application to different biological fluids or health conditions, paving the way for broader use in glucose monitoring and diabetes management.

ACKNOWLEDGMENTS

We would like to acknowledge The Directorate General of Higher Education, Research, and Technology, The Ministry of Education, Culture, Research and Technology, Republic of Indonesia, for the research funding in scheme Penelitian Pascasarjana fiscal year 2024 with contract number 027/E5/PG.02.00.PL/2024 and 22323/IT3.D10/PT.01.03/P/B/2024.

REFERENCES

1. Tang L, Chang SJ, Chen CJ, Liu JT. Non-invasive blood glucose monitoring technology: A review. *Sensors (Switzerland)*. 2020;20(23):1-32. doi:10.3390/s20236925
2. Bruen D, Delaney C, Florea L, Diamond D. Glucose sensing for diabetes monitoring: Recent developments. *Sensors (Switzerland)*. 2017;17(8). doi:10.3390/s17081866
3. Oliver JD, Rosser AA, Fellows CM, et al. Understanding and improving direct UV detection of monosaccharides and disaccharides in free solution capillary electrophoresis. *Anal Chim Acta*. 2014;809:183-193. doi:10.1016/j.aca.2013.12.001
4. Chen X, Chen J, Wang F, et al. Determination of glucose and uric acid with bienzyme colorimetry on microfluidic paper-based analysis devices. *Biosens Bioelectron*. 2012;35(1):363-368. doi:10.1016/j.bios.2012.03.018
5. Prasad SN, Weerathunge P, Karim N, et al. Non-invasive detection of glucose in human urine using a color-generating copper NanoZyme. Published online 2021:1279-1291.
6. Yang D, Luo M, Di J, Tu Y, Yan J. Gold nanocluster-based ratiometric fluorescent probes for hydrogen peroxide and enzymatic sensing of uric acid. *Microchimica Acta*. 2018;185(6). doi:10.1007/s00604-018-2823-5
7. Serafim JA, Silveira RF, Vicente EF. Fast Determination of Short-Chain Fatty Acids and Glucose Simultaneously by Ultraviolet/Visible and Refraction Index Detectors via High-Performance Liquid Chromatography. *Food Anal Methods*. 2021;14(7):1387-1393. doi:10.1007/s12161-021-01990-w
8. Anderson K, Poulter B, Dudgeon J, Li SE, Ma X. A highly sensitive nonenzymatic glucose biosensor based on the regulatory effect of glucose on electrochemical behaviors of colloidal silver nanoparticles on MoS2. *Sensors (Switzerland)*. 2017;17(8). doi:10.3390/s17081807
9. Ayranci R, Demirkan B, Sen B, Aysun Ş, Ak M, Fatih Ş. Materials Science & Engineering C Use of the monodisperse Pt / Ni @ rGO nanocomposite synthesized by ultrasonic hydroxide assisted reduction method in electrochemical nonenzymatic glucose detection. 2019;99(February):951-956. doi:10.1016/j.msec.2019.02.040
10. Soleh A, Kanatharana P, Thavarungkul P, Limbut W. Novel electrochemical sensor using a dual-working electrode system for the simultaneous determination of glucose, uric acid and dopamine. *Microchemical Journal*. 2020;153(August 2019):104379. doi:10.1016/j.microc.2019.104379
11. Golsanamlou Z, Mahmoudpour M, Soleymani J, Jouyban A. Applications of Advanced Materials for Non-Enzymatic Glucose Monitoring: From Invasive to the Wearable Device. *Crit Rev Anal Chem*. 2023;53(5):1116-1131. doi:10.1080/10408347.2021.2008227
12. Franco FF, Hogg RA, Manjakkal L. Cu2 O-Based Electrochemical Biosensor for Non-Invasive and Portable Glucose Detection. *Biosensors (Basel)*. 2022;12(3):1-11. doi:10.3390/bios12030174
13. Singh B, Laffir F, McCormac T, Dempsey E. PtAu/C based bimetallic nanocomposites for non-enzymatic electrochemical glucose detection. *Sens Actuators B Chem*. 2010;150(1):80-92. doi:10.1016/j.snb.2010.07.039
14. Gao J, He S, Nag A. Electrochemical detection of glucose molecules using laser-induced graphene sensors: A review. *Sensors*. 2021;21(8). doi:10.3390/s21082818
15. Hassan MH, Vyas C, Grieve B, Bartolo P. Recent advances in enzymatic and non-enzymatic electrochemical glucose sensing. *Sensors*. 2021;21(14). doi:10.3390/s21144672
16. Wang F, Shi F, Li J, et al. Cu microspheres decorated ZnO@CNT/Carbon cloth flexible biosensor for simultaneous determination of glucose and uric acid. *Microchemical Journal*. 2023;193(July):109054. doi:10.1016/j.microc.2023.109054
17. Lee H, Hong YJ, Baik S, Hyeon T, Kim DH. Enzyme-Based Glucose Sensor: From Invasive to Wearable Device. *Adv Healthc Mater*. 2018;7(8):1-14. doi:10.1002/adhm.201701150
18. Shokrekhodaei M, Quinones S. Review of non-invasive glucose sensing techniques: Optical,

electrical and breath acetone. *Sensors (Switzerland)*. 2020;20(5). doi:10.3390/s20051251

19. Xu L, Zhao R, Zhao Y, et al. Genetic and clinical characterization of familial renal glucosuria. *Clin Kidney J*. 2024;17(2). doi:10.1093/ckj/sfad265
20. Russell WR, Baka A, Björck I, et al. Impact of Diet Composition on Blood Glucose Regulation. *Crit Rev Food Sci Nutr*. 2016;56(4):541-590. doi:10.1080/10408398.2013.792772
21. Baig N, Sajid M, Saleh TA. SC. *Trends in Analytical Chemistry*. Published online 2018. doi:10.1016/j.trac.2018.11.044
22. Hwang DW, Lee S, Seo M, Chung TD. Recent advances in electrochemical non-enzymatic glucose sensors – A review. *Anal Chim Acta*. 2018;1033:1-34. doi:10.1016/j.aca.2018.05.051
23. Toghill KE, Compton RG. Electrochemical non-enzymatic glucose sensors: A perspective and an evaluation. *Int J Electrochem Sci*. 2010;5(9):1246-1301. doi:10.1016/s1452-3981(23)15359-4
24. Woo H, Lee HJ, Yook JG. Noninvasive Detection of Glucose and NaCl Solutions With Environment Correction Using a Dual IDC-Based Microwave Sensor. *IEEE Sens J*. 2024;24(12):19039-19049. doi:10.1109/JSEN.2024.3390544
25. Lee SJ, Sung YG, Kesavan S, Kim CL. Development of highly sensitive/durable porous carbon nanotube–polydimethylsiloxane sponge electrode for wearable human motion monitoring sensor. *New J Chem*. 2024;48(5):2146-2154. doi:10.1039/D3NJ04802K
26. Mohamad Nor N, Ridhuan NS, Abdul Razak K. Progress of Enzymatic and Non-Enzymatic Electrochemical Glucose Biosensor Based on Nanomaterial-Modified Electrode. *Biosensors (Basel)*. 2022;12(12). doi:10.3390/bios12121136
27. Naikoo GA, Salim H, Hassan IU, et al. Recent Advances in Non-Enzymatic Glucose Sensors Based on Metal and Metal Oxide Nanostructures for Diabetes Management- A Review. *Front Chem*. 2021;9. doi:10.3389/fchem.2021.748957
28. Dhara K, Mahapatra DR. *Electrochemical Nonenzymatic Sensing of Glucose Using Advanced Nanomaterials*. Vol 185. Microchimica Acta; 2018. doi:10.1007/s00604-017-2609-1
29. Xie F, Yang M, Jiang M, Huang XJ, Liu WQ, Xie PH. Carbon-based nanomaterials – A promising electrochemical sensor toward persistent toxic substance. *TrAC - Trends in Analytical Chemistry*. 2019;119. doi:10.1016/j.trac.2019.115624
30. Ismail MS, Yusof N, Mohd Yusop MZ, et al. Synthesis and characterization of graphene derived from rice husks. *Malaysian Journal of Fundamental and Applied Sciences*. 2019;15(4):516-521. doi:10.11113/mjfas.v15n4.1228
31. Asif M, Aziz A, Wang H, et al. Superlattice stacking by hybridizing layered double hydroxide nanosheets with layers of reduced graphene oxide for electrochemical simultaneous determination of dopamine, uric acid and ascorbic acid. *Microchimica Acta*. 2019;186(2). doi:10.1007/s00604-018-3158-y
32. Putra BR, Nisa U, Heryanto R, et al. A facile electrochemical sensor based on a composite of electrochemically reduced graphene oxide and a PEDOT:PSS modified glassy carbon electrode for uric acid detection. *Analytical Sciences*. 2022;38(1):157-166. doi:10.2116/analsci.21P214
33. Akhavan O, Bijanzad K, Mirsepah A. Synthesis of graphene from natural and industrial carbonaceous wastes. *RSC Adv*. 2014;4(39):20441-20448. doi:10.1039/c4ra01550a
34. Habte AT, Ayele DW, Hu M. Synthesis and Characterization of Reduced Graphene Oxide (rGO) Started from Graphene Oxide (GO) Using the Tour Method with Different Parameters. *Advances in Materials Science and Engineering*. 2019;2019(Vc). doi:10.1155/2019/5058163
35. Sasaki KI, Tokura Y, Sogawa T. The origin of Raman D band: Bonding and antibonding orbitals in graphene. *Crystals (Basel)*. 2013;3(1):120-140. doi:10.3390/cryst3010120
36. Bîru EI, Iovu H. Graphene Nanocomposites Studied by Raman Spectroscopy. *Raman Spectroscopy*. Published online 2018. doi:10.5772/intechopen.73487
37. Gurunathan S, Jeyaraj M, Kang MH, Kim JH. Graphene oxide-platinum nanoparticle nanocomposites: A suitable biocompatible therapeutic agent for prostate cancer. *Polymers (Basel)*. 2019;11(4). doi:10.3390/polym11040733
38. Botello LE, Schönig M, Solla-Gullón J, Climent V, Feliu JM, Schuster R. Direct measurement of the hydrogen adsorption entropy on shape-controlled Pt nanoparticles using electrochemical microcalorimetry. *J Mater Chem A*. 2024;12(1):184-191. doi:10.1039/D3TA04937J

39. Saravanan G, Mohan S. Pt nanoparticles embedded on reduced graphite oxide with excellent electrocatalytic properties. *Appl Surf Sci*. 2016;386:96-102. doi:10.1016/j.apsusc.2016.05.152
40. Mazzotta E, Caroli A, Primiceri E, Monteduro AG, Maruccio G, Malitesta C. All-electrochemical approach for the assembly of platinum nanoparticles/polypyrrole nanowire composite with electrocatalytic effect on dopamine oxidation. *Journal of Solid State Electrochemistry*. 2017;21(12):3495-3504. doi:10.1007/s10008-017-3693-1
41. Wang P, Olbricht WL. Study on electrodeposition of Pt. *Surface Engineering*. 2011;27(9):662-670. doi:10.1179/1743294410Y.0000000007
42. Kokoskarova P, Stojanov L, Najkov K, et al. Square-wave voltammetry of human blood serum. *Sci Rep*. 2023;13(1). doi:10.1038/s41598-023-34350-1
43. Yang QQ, He S, Zhang YL, et al. A colorimetric sensing strategy based on chitosan-stabilized platinum nanoparticles for quick detection of α-glucosidase activity and inhibitor screening. *Anal Bioanal Chem*. Published online February 15, 2024. doi:10.1007/s00216-024-05198-9
44. Bard AJ., Faulkner LR. *Electrochemical Methods : Fundamentals and Applications*. John Wiley & Sons, Inc.; 2001.
45. Kumar MA, Lakshminarayanan V, Ramamurthy SS. Platinum nanoparticles–decorated graphene-modified glassy carbon electrode toward the electrochemical determination of ascorbic acid, dopamine, and paracetamol. *Comptes Rendus Chimie*. 2019;22(1):58-72. doi:10.1016/j.crci.2018.09.015
46. Ma W, Hu K, Chen Q, Zhou M, Mirkin M V., Bard AJ. Electrochemical Size Measurement and Characterization of Electrodeposited Platinum Nanoparticles at Nanometer Resolution with Scanning Electrochemical Microscopy. *Nano Lett*. 2017;17(7):4354-4358. doi:10.1021/acs.nanolett.7b01437
47. Danaee I, Jafarian M, Forouzandeh F, Gobal F. Kinetic studies of glucose electrocatalytic oxidation on GC/Ni electrode. *Int J Chem Kinet*. 2012;44(11):712-721. doi:10.1002/kin.20721
48. Karim-Nezhad G, Hasanzadeh M, Saghatforoush L, Shadjou N, Earshad S, Khalilzadeh B. Kinetic Study of Electrocatalytic Oxidation of Carbohydrates on Cobalt Hydroxide Modified Glassy Carbon Electrode. *J Braz Chem Soc*. 2009;20(1):141-151. doi:10.1590/S0103-50532009000100022
49. Calcagno D, Perina ML, Zingale GA, et al. Detection of insulin oligomeric forms by a novel surface plasmon resonance-diffusion coefficient based approach. *Protein Science*. 2024;33(4):e4962. doi:https://doi.org/10.1002/pro.4962
50. Wu M, Li L, Yu R, et al. Tailored diffusion limiting membrane for microneedle glucose sensors with wide linear range. *Talanta*. 2024;273:125933. doi:https://doi.org/10.1016/j.talanta.2024.125933
51. Moldenhauer J, Meier M, Paul DW. Rapid and Direct Determination of Diffusion Coefficients Using Microelectrode Arrays. *J Electrochem Soc*. 2016;163(8):H672-H678. doi:10.1149/2.0561608jes
52. Yin W. Urine Glucose Levels Are Disordered Before Blood Glucose Levels Increase In Zucker Diabetic Fatty Rats. Published online 2017. doi:10.1101/122283
53. Boorsma EM, Beusekamp JC, ter Maaten JM, et al. Effects of empagliflozin on renal sodium and glucose handling in patients with acute heart failure. *Eur J Heart Fail*. 2021;23(1):68-78. doi:10.1002/ejhf.2066
54. Wahyuni WT, Safitri H, Rohaeti E, Khalil M, Putra BR. A Novel Approach to Fabricating a Screen-Printed Electrode Based on a Gold Nanorod–Graphene Oxide Composite for the Detection of Uric Acid †. *Engineering Proceedings*. 2023;48(1):1-9. doi:10.3390/CSAC2023-14908
55. Wei G, Xu F, Li Z, Jandt KD. Protein-promoted synthesis of Pt nanoparticles on carbon nanotubes for electrocatalytic nanohybrids with enhanced glucose sensing. *Journal of Physical Chemistry C*. 2011;115(23):11453-11460. doi:10.1021/jp202324q
56. Kogularasu S, Lee YY, Chang-Chien GP, Chen PY, Govindasamy M. A Novel Synthesis of Nickel Carbide Modified Glassy Carbon Electrode for Electrochemical Investigation of Archetypal Diabetes Biomarker in Human Serum and Urine Samples. *J Electrochem Soc*. 2024;171(4):47512. doi:10.1149/1945-7111/ad3a21
57. M. P. A, R. A, Haridas S. Selective and sensitive non-enzymatic detection of glucose by Cu(ii)–Ni(ii)/SBA-15. *New J Chem*. 2024;48(12):5326-5333. doi:10.1039/D4NJ00039K
58. Bano M, Naikoo GA, BaOmar F, et al. Revolutionizing Glucose Monitoring:

Enzyme-Free 2D-MoS2 Nanostructures for Ultra-Sensitive Glucose Sensors with Real-Time Health-Monitoring Capabilities. *ACS Omega*. 2024;9(18):20021-20029. doi:10.1021/acsomega.3c10117

59. Mekersi M, Ferkhi M, Kuyumcu Savan E. Electrochemical biodetection of glucose using La0.6Sr0.4Co0.8Fe0.2O3 and La1,7Sr0,3CuO4 Nano-Particles modified with black carbon deposited on glassy carbon electrode. *Microchemical Journal*. 2023;194:109346. doi:https://doi.org/10.1016/j.microc.2023.109346
60. Sun E, Gu Z, Li H, Liu X, Li Y, Xiao F. Flexible Graphene Paper Modified Using Pt&Pd Alloy Nanoparticles Decorated Nanoporous Gold Support for the Electrochemical Sensing of Small Molecular Biomarkers. *Biosensors (Basel)*. 2024;14(4). doi:10.3390/bios14040172
61. Bhuvaneswari C, Elangovan A, Sudhan N, et al. A low-cost hybrid GQDs/Fe3O4/polypyrrole nanocomposite based chemo-sensor for electrochemical non-enzymatic selective determination of creatinine in biological samples. *Microchemical Journal*. 2023;194:109259. doi:https://doi.org/10.1016/j.microc.2023.109259
62. Rashed MdA, Nayem N, Rahman MH, et al. A sensitive, selective non-enzymatic electrochemical detection and kinetic study of glucose over Pt nanoparticles/SWCNTs/NiO ternary nanocomposite. *J Taiwan Inst Chem Eng*. 2023;151:105113. doi:https://doi.org/10.1016/j.jtice.2023.105113